20 mm 厚 6063 铝合金搅拌摩擦焊焊缝 S 曲线控制

贺地求，　叶绍勇，　汪　建
（中南大学 高性能复杂制造国家重点实验室，长沙　410083）

贺地求

摘　要： 针对 6063 铝合金搅拌摩擦焊缝中易出现“S”曲线的问题，在采用搅拌摩擦焊焊接 20 mm 厚 6063 铝合金散热器的过程中，使用气体保护，成功消除了 6063 铝合金搅拌摩擦焊中易形成的“S”曲线，获得了成形良好的焊缝组织，焊缝的平均抗拉强度达到 148.83 MPa，焊接强度系数为母材的 81.9%. 通过分析焊缝的微观组织，发现焊核区发生了完全动态再结晶，组织为细小的等轴晶粒. 热力影响区发生明显塑性变形，发生不同程度的动态再结晶，晶粒发生明显长大. 热影响区受焊接热循环影响，发生了微观组织和力学性能变化，但没有发生塑性变形，晶粒发生粗化.

关键词： 搅拌摩擦焊；6063 铝合金；S 曲线；显微组织
中图分类号： TG453　　**文献标识码：** A　　**文章编号：** 0253－360X(2013)12－0021－04

0　序　　言

6063(LD31)为 Al-Mg-Si 系锻铝性合金，强度中等，塑性较好，热导率高，因此在型材制造中得到广泛应用[1]. 由于挤压型材设备有限，大型的铝合金挤压型材采用焊接等方法拼接. 但是采用熔焊方法焊接铝合金材料存在许多问题，如对零件表面氧化膜敏感、裂纹倾向大、易产生气孔等[2,3]. 金属固态焊接方法搅拌摩擦焊(friction stir welding，FSW)，能够避免因接头金属熔化造成的气孔、裂纹等冶金缺陷，因此在铝合金、镁合金等轻合金焊接等方面中得到广泛应用[4].

6063 铝合金搅拌摩擦焊接过程中，容易在接头横截面出现呈 S 状的黑色曲线研究者称之为“S”曲线的缺陷. Di 等人[5] 对 4 mm 厚的 AA2024-T4 进行了 FSW，认为 S 曲线是 FSW 接头中一种特殊的根部缺陷，对接头疲劳寿命产生了直接的影响，疲劳强度从 96.19 MPa 下降到 73.71 MPa，降低了 23.4%. 刘耀等人[6] 研究了 4 mm 厚 LF6 铝合金 FSW 焊后拉伸性能，拉伸断口呈 S 形，平均抗拉强度下降了 10.5%. 焊接工艺参数选取不当时，由于氧化膜的存在，底部对接面上的金属只是因塑性变形而紧贴在一起，没有达到原子间的结合.

Liu 等人[7] 研究了 Al-Cu 合金的 S 曲线，认为“S”曲线对焊后热处理的接头有破坏性的影响.

收稿日期： 2012－05－10
基金项目： 国家“973”高科技资助项目(2010CB731704)

6063 铝合金散热器有由于其本身特有的高效散热结构，其散热面积是 20 mm 平板的 6 倍左右，且焊接厚度达到 20 mm，在焊接过程中，焊缝上下易形成大的温度梯度. 在实际焊接过程中，采用焊前去除对接面氧化皮，提高旋转频率增大热输入量，都不能消除“S”曲线，说明“S”曲线可能是在焊接过程形成. 文中针对 6063 铝合金散热器 FSW 焊接中容易形成“S”曲线的问题，采用带氩气的保护方式进行搅拌摩擦焊，有效消除了“S”曲线，获得了无缺陷、成形良好的焊缝，并分析了焊缝的组织性能.

1　试验方法

试验材料为 6063-T5(Al-Mg-Si 系)铝合金，热处理状态为 T5，6063-T5 铝合金化学成分见表 1. 焊前对散热器接头部分表面进行清洗，去除氧化皮，防止氧化皮在焊接过程中被打碎搅入焊缝，对焊缝产生影响. 焊接过程中在焊缝底部通入足量的 0.1 MPa 氩气，保证两个散热器对接缝隙中无氧气. 试验用搅拌头参数为搅拌头轴肩直径 35 mm，搅棒针直径 13 mm，长度 19.5 mm，略小于板材厚度. 焊接工艺参数为搅拌头旋转频率 1 400 r/min，搅拌头沿焊缝方向的焊接速度 55 mm/min.

表 1　6063-T5 铝合金主要化学成分(质量分数，%)
Table 1　Chemical compositions of 6063-T5 Al alloy

Mg	Si	Fe	Cu	Mn	Al
0.6	0.4	0.25	0.10	0.15	余量

焊接后分别进行拉伸试验和金相试验. 焊接完成后,沿焊缝横向截取 6 个拉伸试样进行拉伸试验,拉伸试验在 DDL100 电子万能试验机上进行,试样尺寸见图 1. 制成金相试样后,用 0.5% HF 溶液对抛光后的试样进行腐蚀,在光学显微镜下对焊缝微观组织进行观察.

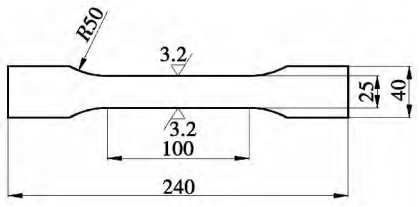

图 1 拉伸试样尺寸(mm)

Fig. 1 Shape and size of tensile test specimens

2 试验结果及分析

2.1 接头力学性能

在上述工艺参数下得到的 6063-T5 焊缝力学性能见表 2. 从试验结果可见,在未经任何焊后热处理时,20 mm 的 6063-T5 铝合金搅拌摩擦焊焊缝的平均抗拉强度达到了 148.83 MPa,焊缝强度达到了母材的 81.9%.

表 2 6063-T5 铝合金 20 mm 板焊缝拉伸试验结果

Table 2 Mechanical properties of 6063-T5 FSW

编号	抗拉强度 R_m/MPa	断后伸长率 A(%)
1	153	18.0
2	145	17.0
3	143	19.0
4	151	18.0
5	150	17.6
6	151	18.0
平均值	149	17.9

拉伸试样断裂外观形貌如图 2 所示,断裂位置均发生在焊缝的返回侧,位于热力影响区与热影响区的交界处,断裂方向与应力方向成 45°. 相关研究[8,9]表明由于金属材料塑性流动不完全,前进侧易产生孔洞等缺陷,焊缝的薄弱处一般位于前进侧. 断裂位置发生在返回侧与焊件本身所特有的高效散热结构有关. 从图 3 宏观形貌中看到,焊缝前进侧对应有两个翅片,返回侧对应只有一个翅片,前进侧的散热强度大于返回侧. 要保证获得良好的焊缝,需要大的热量输入,当前进侧获得的热量合适时,返回侧温度会远高于前进侧,也高于平板搅拌摩擦焊返回侧温度. 返回侧材料在高温下,晶粒发生长大,导致强度下降. 这一点在金相组织观察中得到了验证.

图 2 拉伸试样断裂形貌

Fig. 2 Tensile specimens fracture morphology

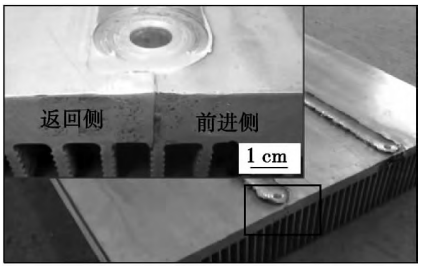

图 3 焊缝宏观形貌

Fig. 3 Macrophotograph of welding joint

2.2 断口分析

从焊缝拉伸断口微观形貌(图 4)可以看出,焊缝断口中存在较大较深的等轴韧窝和撕裂棱,焊缝具有较好的韧性,为韧性断裂. 在断口上还可以看到部分细小的第二相粒子剥离后留下的非常细小的光滑韧窝,说明存在部分沿晶断裂. 由此可见,焊缝的整体断裂形式为以韧性断裂为主的韧/脆混合型断裂,由此也可以看出焊缝具有较好的延性.

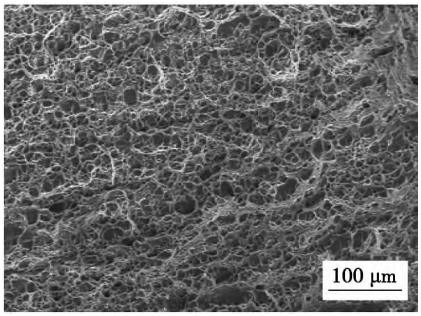

图 4 焊缝拉伸断口微观形貌

Fig. 4 Tensile fracture morphologies of FSW joint

2.3　金相组织分析

图 5 为焊缝中 3 个区的高倍金相微观组织，在 3 个区中未发现孔洞、组织疏松、热裂纹、S 曲线等缺陷. 图 5a，b 分别为焊缝底部和上部的焊核区(weld nugget zone，WNZ) ，其中焊缝上部的焊核区组织晶界连续闭合，晶粒较小，焊缝底部的焊核区组织的晶界不连续，晶粒尺寸更加细小. 焊核区组织在搅拌头强烈的机械搅拌作用以及轴肩与工件剧烈摩擦产生局部高温的共同作用下，造成大量晶粒破碎，破碎的晶粒发生动态再结晶，形成细小等轴晶粒. 但是由于搅拌摩擦焊的特点，轴肩与搅拌针的摩擦产热机制导致焊接区域形成上热下冷的漏斗状温度分布. 上部区域较底部区域能获得持续时间更长、更高的温度，破碎的晶粒发生了充分的动态再结晶. 而底部形成不连续的晶界，并且由于高温时间较短，其再结晶晶粒来不及长大，晶粒更为细小. 图 5c，d 为热力影响区(TMAZ) 组织，热力影响区的晶粒受到搅拌头轴肩的挤压作用，晶粒被拉长，但晶粒变形没有焊核区剧烈. 前进侧与返回侧晶粒形状尺寸相差较大，前进侧晶粒沿流动方向被拉长成窄条状组织，而在返回侧晶粒被拉伸成扁平块状. 这是由于在前进侧，焊缝金属塑性流动方向与母材金属塑性流动方向相反，使母材金属与焊缝金属之间存在很大的相对变形差，在返回侧焊缝金属塑性流动方向与母材金属塑性流动方向相同[10]. 返回侧的晶粒比较粗大，这是由于焊缝处翅片分布导致返回侧热量累积，温度高于前进侧，再结晶晶粒在持续高温下发生长大，这也证明了焊缝的薄弱处位于返回侧；图 5e 为热影响区(HAZ) ，热影响区没有受到搅拌头的机械搅拌作用，但在焊接过程中受到了热循环作用，导致该区域内组织发生一定的长大粗化. 图 5f 为母材(parent mateial，PM) 金相组织形貌，母材呈轧制状粗大晶粒.

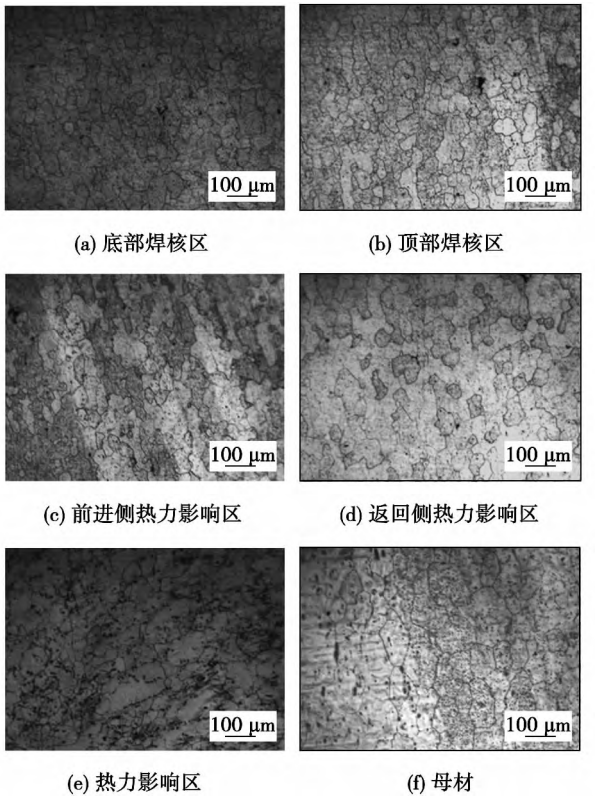

图 5　6063-T5 焊缝的微观组织

Fig. 5　Microstructure of 6063-T5 FSW joint

3　结　　论

(1) 6063-T5 铝合金散热器 S 曲线的形成主要是由于焊缝对接面存在空气，铝在焊接过程中被氧化而形成致密的氧化膜；在焊接过程中增加气体保护，使对接面与氧气隔绝能够有效的阻止氧化膜的形成，消除 S 曲线.

(2) 搅拌头的旋转频率为 1 400 r/min，焊接速度为 55 mm/min 时，焊缝的平均抗拉强度达到了 148.83 MPa，焊缝强度达到了母材的 81.9%.

(3) 散热器翅片在焊缝周围的分布情况会影响焊接中焊缝区的热量分布，进而对 6063-T5 铝合金散热器焊缝拉伸断裂位置产生影响.

(4) 6063-T5 搅拌摩擦焊得到了良好的焊缝组织，焊缝组织根据形状和大小，可明显分为焊核区(WNZ) ，热力影响区(TMAZ) 和热影响区(HAZ) .

参考文献：

[1] 林　钢，林慧国，赵玉涛. 铝合金应用手册 [M]. 北京：机械工业出版社，2006.

[2] 黄旺福，黄金刚. 铝及铝合金焊接指南 [M]. 湖南：湖南科学技术出版社，2004.

[3] 柴　鹏，简　波，季亚娟，等. 6063 铝合金搅拌摩擦焊接头冲击断裂分析 [J]. 焊接学报，2005，26(9) ：27 - 30.
Chai Peng，Jian Bo，Ji Yajuan，*et al*. Impact properties of 6063 Al alloy FSW weld [J]. Transactions of the China Welding Institution，2005，26(9) ：27 - 30.

[4] Mishra R S，Ma Z Y. Friction stir welding and processing [J]. Materials Science and Engineering R，2005，50：1 - 78.

[5] Di Shusheng，Yang Xinqi，Luan Guohong，*et al*. Comparative study on fatigue prosperities between AA2024-T4 friction stir welds and base materials [J]. Materials Science and Engineering A，2006，435/436，389 - 395.

[6] 刘　耀，邢　丽，杨成刚，等. LF6 铝合金搅拌摩擦焊焊缝中 S 曲线对接头拉伸性能的影响 [J]. 热加工工艺，2010，39(17) ：139 - 141.

Liu Yao, Xing Li, Yang Chenggang, *et al*. Influence of S-type curve in friction stir welds on tensile properties of welded joint of aluminum alloy LF6 [J]. Hot Working Technology, 2010, 39(17): 139 - 141.

[7] Liu Huijie, Chen Yingchun, Feng Jicai. Effect of zigzag line on the mechanical properties of friction stir welded joints of Al-Cu alloy [J]. Scripta Materialia, 2006(55): 231 - 234.

[8] 王希靖, 孙桂芳. 7075 铝合金搅拌摩擦焊接头组织及性能 [J]. 宇航材料工艺, 2008, 38(6): 77 - 80.
Wang Xijing, Sun Guiping. Microstructure and properties of friction stir welding joints for 7075 aluminum alloy [J]. Aerospace Materials & Technology, 2008, 38(6): 77 ~ 80.

[9] 赵衍华, 林三宝, 吴 林. 2014 铝合金搅拌摩擦焊接过程塑性金属流变可视化 [J]. 焊接学报, 2005, 26(6): 73 - 76.
Zhao Yanhua, Lin Sanbao, Wu Lin. Visualization of material flow in 2014 Al alloy friction stir welding process [J]. Transactions of the China Welding Institution, 2005, 26(6): 73 - 76.

[10] 邢 丽, 陈爱华, 刘鸽平, 等. 焊接参数对 LY12 铝合金 FSW 焊缝 S 曲线形成的影响 [J]. 焊接学报, 2010, 31(5): 9 - 12.
Xing Li, Chen Aihua, Liu Geping, *et al*. Effects of welding parameters on formation of lazy S weld in friction stir welding of LY12 Al-alloy [J]. Transactions of the China Welding Institution, 2010, 31(5): 9 - 12.

作者简介: 贺地求, 男, 1963 年出生, 硕士, 教授, 硕士研究生导师. 主要从事搅拌摩擦焊工艺和机理研究. 发表论文 20 余篇.
Email: hdqzzp@163.com.

书 讯

书号: 978-7-111-37251-6
定价: 49.00元

《异种金属的焊接》

作者: 史春元 于启湛 编著

随着制造业的发展和产业需求的多元化, 对材料也提出了更高、更复杂的要求。既要满足设备的实际需求, 又要降低成本, 达到经济效益的最大化。要满足这些要求, 往往不是一种材料所能实现的。异种材料焊接是制造业发展过程中必然会遇到的问题, 技术难度较大, 焊接过程也十分复杂。

本书简要地介绍了异种金属材料的焊接性; 较详细地讨论了异种钢之间、异种非铁金属之间、钢与非铁金属之间、双金属或多金属复合板之间的焊接等。

本书可供高等院校焊接专业师生、科研机构的焊接研究人员、新产品制造和维修的技术人员参考。

Wensheng, CAI Qingshan (State Key Laboratory for Powder Metallurgy, Central South University, Changsha 410083, China). pp 17 – 20

Abstract: The interface characteristics between W and ferrite steel (FS) diffusion welded with a V interlayer of 0.5mm in thickness was investigated in vacuum hot pressing furnace at 1 050 ℃ for 1h and 10 MPa. Microstructures, element compositions and micro-hardness of joint were analyzed and tested with field-emission scanning electron microscopy (FE-SEM), energy dispersive spectroscopy (EDS) and nanoindenter, respectively. Tensile strength was tested with mechanical test machine. Results showed that, a reliable bonding on W/FS interfaces by means of diffusion welding between matrix and V interlayer was obtained. The W/FS joint is a multilayer sandwich structure, which includes the transition zone of W/V, the residual V interlayer and the diffusion layer of V/FS. Meanwhile, the transition zone of W/V was mainly composed of a solid solution structure and the V/FS diffusion layer with the highest hardness where there was a definite structure of V/VC layer/decarburized layer/FS. The tensile strength of joint reaches 75MPa and V/FS interface is main fracture source because of containing brittle VC phase.

Key words: tungsten; steel; diffusion bonding; interlayer; microstructure

Elimination of lazy S defect in friction stir welded joint of 20mm-6063 alumimum alloy HE Diqiu, YE Shaoyong, WANG Jian (State Key Laboratory of Complicated Equipment Design and Extreme Manufacturing, Central South University, Changsha 410083, China). pp 21 – 24

Abstract: 20 mm thick 6063 aluminum alloy plate were joined by friction stir welding with gas protection. The result showed that the sound joint without lazy S can be achieved. The average tensile strength of welds is 148.9 MPa, which is 81.9% of that of the base metal. Optical microscopy revealed the stir zone presents particularly fined equiaxed gains formed by dynamic recrystallization. The microstructure in TMAZ, in which some degree of dynamic recrystallization occurs, consists of deformed gains. The result shows that lazy S of 6063 aluminum alloy can be eliminated by FSW with gas protection.

Key words: friction stir welding; 6063 aluminum alloy; lazy S; microstructure

A novel method of in-situ fabrication of Mg surface composites by friction stir process HUANG Yongxian[1], WANG Tianhao[1], LÜ Shixiong[1], LIU Huijie[1], AO Feng[2] (1. State Key Laboratory of Advanced Welding and Joining, Harbin Institute of Technology, Harbin 150001, China; 2. Yangzhou Qiuyuan Pressure Vessel Manufacturing Co., Ltd., Yangzhou 225115, China). pp 25 – 28

Abstract: In the previous fabrication process of surface composite by friction stir process (FSP), the reinforcement phases were needed to preplace on the base metal. However, these particles didn't distribute very well in the stir zone. Therefore, friction stir process without preplacing reinforcement phase was proposed to prepare the surface composite. A FSP tool consisting of only shoulder was designed, and used to fabricate the surface composite on the AZ31 plate as-rolled. Microstructure was analyzed by optical microscope and SEM. The microhardness and surface wear resistance tests of specimens show that the particle reinforcement are more homogeneous, so that the microhardness and wear resistance increase, and at the same time, the preparation work is simplified to a great extent.

Key words: magnesium alloy; friction stir process; in-situ; surface composites

Characteristics of bypass-current MIG-TIG double-sided welding of stainless steel MIAO Yugang[1], HAN Duanfeng[1], WU Bintao[2], XU Xiangfang[2], LI Xiaoxu[2] (1. National Key Laboratory of Science and Technology on Underwater Vehicle, Harbin Engineering University, Harbin 150001, China; 2. College of Shipbuilding Engineering, Harbin Engineering University, Harbin 150001, China). pp 29 – 32

Abstract: By using 6mm thick 304 stainless steel plate as base metal, the bypass-current double-sided arc welding experiments were carried out. The results showed the technology can obtain the stable process and good weld appearance. The other remarkable advantages such as increasing joint penetration, deceasing welding defects, enhancing production efficiency, reducing welding cost were also achieved. The reliable joining of 6mm thick 304 stainless steel was realized at welding current of 110 A. Furthermore, the melting efficiency of bypass-current double-sided arc welding can reach 60.2%, more than 17.6% of TIG welding and 43.2% of bypass-current MIG welding. The tensile results showed the strength of the joints can reach 776.5MPa, about 95% of that of base metal. The fracture occurs at the heat-effect zone, and the angle between fracture line and stress direction is 45°. The fracture appearance is gray, which shows the characteristics of ductile fracture.

Key words: bypass-current MIG-TIG double-sided welding; melting efficiency; tensile strength; weld appearance

Test and analysis of arc pressure measurement in coupling arc electrode TIG welding HUANG Yong[1,2], HAO Yanzhao[2], QU Huaiyu[2], LIU Ruilin[2] (1. State Key Laboratory of Gansu Advanced Non-ferrous Metal Materials, Lanzhou University of Technology, Lanzhou 730050, China; 2. Key Laboratory of Non-ferrous Metal Alloys and Processing, The Ministry of Education, Lanzhou University of Technology, Lanzhou 730050, China). pp 33 – 36

Abstract: A kind of coupling arc tungsten electrode was developed to decrease arc pressure remarkably, avoid undercut and humping weld. Adopting this method, high-quality TIG welding with relative higher speed can be achieved. The TIG arc pressure of this kind of welding process was tested to investigate the influence of the parameters on distribution of arc pressure. Compared with the traditional TIG arc, the TIG arc pressure with coupling arc electrode is much lower with the same parameters, and decreases with the increase of arc length, the increase of electrode extended length, the decrease of current, the increase of the electrode gap width and the increase of the electrode diameters. The arrangement of the influence in decreasing order is current, electrode extended length, arc length and electrode diameter, electrode gap width.